Physics-Based Deformable Organisms for Medical Image Analysis

Ghassan Hamarneh and Chris McIntosh

School of Computing Science, Simon Fraser University, Burnaby, BC, V5A 1S6, Canada

ABSTRACT

Previously, "Deformable organisms" were introduced as a novel paradigm for medical image analysis that uses artificial life modelling concepts. Deformable organisms were designed to complement the classical bottom-up deformable models methodologies (geometrical and physical layers), with top-down intelligent deformation control mechanisms (behavioral and cognitive layers). However, a true physical layer was absent and in order to complete medical image segmentation tasks, deformable organisms relied on pure geometry-based shape deformations guided by sensory data, prior structural knowledge, and expert-generated schedules of behaviors. In this paper we introduce the use of physics-based shape deformations within the deformable organisms framework yielding additional robustness by allowing intuitive real-time user guidance and interaction when necessary. We present the results of applying our physics-based deformable organisms, with an underlying dynamic spring-mass mesh model, to segmenting and labelling the corpus callosum in 2D midsagittal magnetic resonance images.

Keywords: Medical image analysis, segmentation, deformable models, artificial life,physics-based modeling

1. INTRODUCTION

Due to the important role of medical imaging in the understanding, diagnosis, and treatment of diseases, potentially overwhelming amounts of medical image data are continuously being acquired. This is creating increasing demands for medical image analysis tools that are not only robust and highly-automated, but also intuitive to use and flexible to adapt to different applications. Medical image segmentation in particular remains one of the key tasks indispensable to a wide array of subsequent quantification and visualization goals in medicine including computer-aided diagnosis and statistical shape analysis applications. Several classifications of segmentation techniques exist including edge, pixel, and region-based techniques, clustering, graph theoretic, and model correlation approaches [1–5]. Deformable models for medical image segmentation gained popularity since the introduction of snakes by Terzopoulos *et al* [6, 7]. In addition to physics-based explicit deformable models [8, 9], geometry-based implicit implementations also attracted attention [10–12]. However, deformable models suffered from sensitivity to initialization and low-level parameter settings. Several techniques were proposed to improve segmentation results by controlling model deformations [13, 14] and allowing only feasible deformations to be produced through the incorporation of shape shape knowledge [15–19]. Other knowledge-based techniques were proposed [20,21,22,23,24,25], including agent based segmentation methods [26,27,28,29,30].

Deformable organisms were introduced earlier[31, 32], providing a framework for incorporating contextual knowledge through the adoption of artificial life modelling concepts (Figure 1)[33, 34]. Deformable organisms were designed to complement the classical bottom-up deformable models methodologies with top-down intelligent deformation control mechanisms (Figure 2). Deformable organisms were capable of rejecting local minima by following a schedule of behaviors designed according to knowledge of anatomy and image characteristics. However, a true physics-based layer was absent in the original deformable organisms and in order to complete medical image segmentation tasks, deformable organisms relied on pure geometry-based shape deformations guided by sensory data, prior structural knowledge, and expert-generated schedules of behaviors.

In this paper we extend earlier work on deformable models by making use of a physics-based implementation of the organism's controlled deformations, in order to provide the ability for an expert user to intervene and guide the segmentation in an intuitive manner, if needed.

The remainder of the paper is organized as follows. In section 2 we describe the methods we use to construct our model (section 2.1), perform deformations (section 2.2), model behaviors (section 2.3), perform sensory operations (section2.4), and enable our organisms decision process (section 2.5). Section 3 provides the results

Medical Imaging 2005: Image Processing, edited by J. Michael Fitzpatrick, Joseph M. Reinhardt, Proc. of SPIE Vol. 5747 (SPIE, Bellingham, WA, 2005)
1605-7422/05/$15 · doi: 10.1117/12.594856

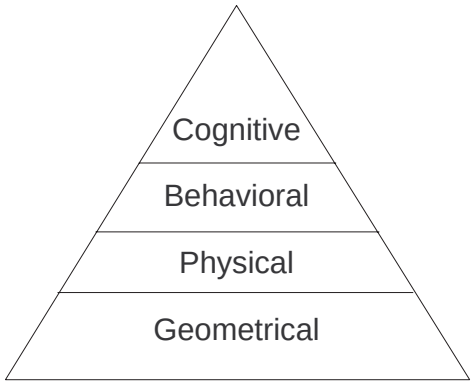

Figure 1. The layered architecture of artificial life modelling used for physics based deformable organisms.

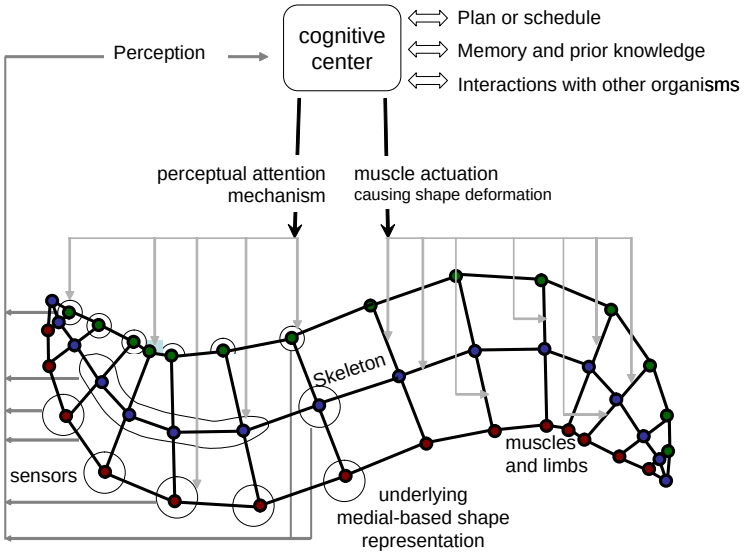

Figure 2. A deformable organism: The brain issues muscle actuation and perceptual attention commands. The organism deforms and senses image features, whose characteristics are conveyed to the brain. The brain makes decisions based on sensory input, memorized information and prior knowledge, and a pre-stored plan, which may involve interaction with other organisms.

of applying our deformable organism to a set of mid-sagittal magnetic resonance images. Our conclusions are presented in section 4, and our acknowledgements in section 5.

2. METHODS

To build the physics-based deformable organism we follow the artificial life layered architecture, composed mainly of geometry, physics, behavior, and cognition layers.

2.1. Geometric Layer

The underlying geometrical shape representation is medial axis-based, in which stretching and bending springs form connections between medial nodes, thickness springs connect medial nodes to boundary nodes, and stabilization springs connect boundary nodes to boundary nodes or medial nodes (Figure 3a). The boundary nodes outline the shape of the organism whereas the medial nodes provide reference points for performing medial-based

deformations. This format is similar to the medial profiles shape representation [35, 36] used in the original deformable organisms [31, 32], however, geometric points and connections are replaced by physics based components as explained in section 2.2.

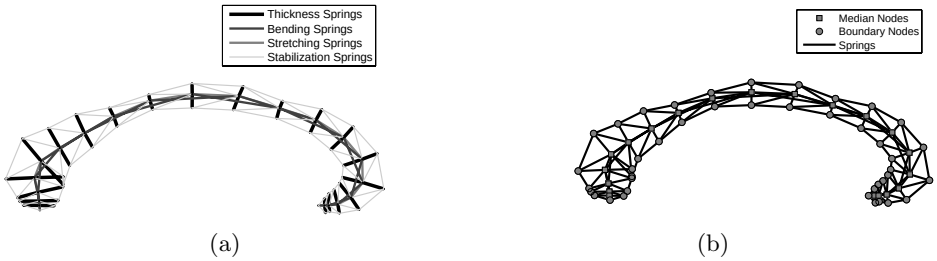

Figure 3. Spring-mass mesh model of the corpus callosum physics-based deformable organism. The figure shows (a) the different types of connecting springs and (b) the medial and boundary masses .

2.2. Physics Layer

In the physics layer, the nodes are modelled as point masses and the connections are modelled as springs (Figure 3b). We adopt the formulation presented in [37] where the organism's deformations are carried out either via internal spring actuation (for scaling, bulging, stretching, and bending) or external forces (for rotation, translation, and user-interaction). Spring actuation are realized via changes in springs' rest lengths while continuously simulating the dynamics via time integration of the organism's motion equation. Statistics on the appropriate ranges for the springs' rest lengths are obtained based on deformation type (e.g. bending vs. bulging) via a hierarchical, regional principal component analysis (Figure 4).

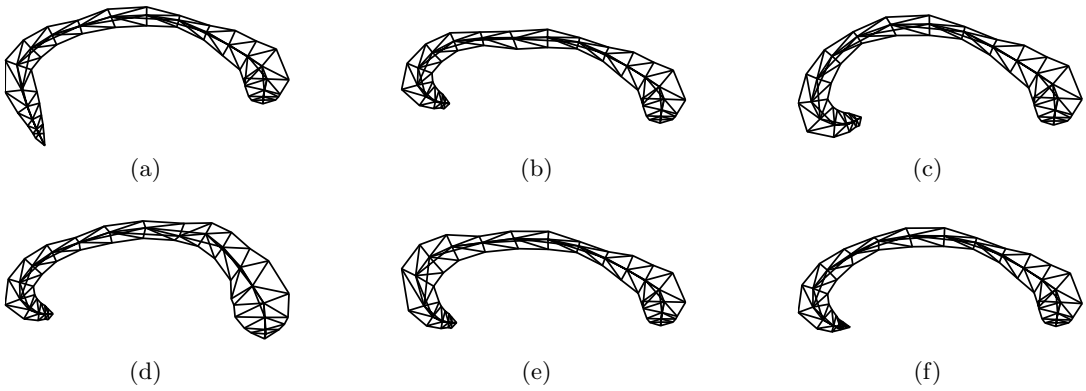

Figure 4. Examples of physics-based deformations of the CC organism using external forces: (a) user applied and (b) rotation forces. Operator based (c) bending, (d) bulging, and (e) stretching deformations. (f) Statistics-based spring actuation.

2.2.1. Dynamic Mesh Model

Let P be an $i\times 2$ matrix containing the 2D coordinates of the i nodes of the model, M a column vector containing the mass for each node, and S a $j\times 2$ matrix that describes which two nodes the *jth* spring connects. Then let K be a column vector consisting of j hook's spring constants, D a column vector of j dampening constants, and R a column vector of j rest lengths. Then A is a matrix of $i\times 2$ accelerations, V a matrix of $i\times 2$ velocities, and F a matrix of $i\times 2$ forces. Finally let E be a vector of i coefficients describing the weight each node gives to external forces. A deformation can now be simulated by applying forces to nodes. From Newton's second law of motion it follows that $A=F./[M\ M]$ where ./ symbolizes an element by element division between two equally sized matrices and $[M\ M]$ denotes the concatenation of M with itself. F is the total force acting on a node at a given time t,

$$F = f_{hook} + f_{viscous} + f_{image} + f_{user} \tag{1}$$

where f_{hook}, $f_{viscous}$, f_{image} and f_{user} are $i \times 2$ matrices containing i 2D spring, viscous, image, and user forces, respectively, and defined as follows.

$$f_{hook,i} = \sum_{u} -K_u(\left\|P_{s_{u,1}} - P_{s_{u,2}}\right\| - R_u)\frac{P_{s_{u,1}} - P_{s_{u,2}}}{\left\|P_{s_{u,1}} - P_{s_{u,2}}\right\|} - \left(D_u\left(V_{s_{u,1}} - V_{s_{u,2}}\right)^T \frac{P_{s_{u,1}} - P_{s_{u,2}}}{\left\|P_{s_{u,1}} - P_{s_{u,2}}\right\|}\right)\frac{P_{s_{u,1}} - P_{s_{u,2}}}{\left\|P_{s_{u,1}} - P_{s_{u,2}}\right\|} \tag{2}$$

$$f_{viscous,i} = \sum_{u} K_u V_i \tag{3}$$

$$f_{image,i} = E_i \nabla\left(\|\nabla I(P_i)\|\right) \tag{4}$$

where u ranges across all springs that originate at a given node i, $P_{s_{u,1}}$ refers to the $S_{u,1}th$ member of P, and $I(P_i)$ refers to the intensity of the image at the location of the ith node. Once the total force at each node is known, we can calculate the new acceleration, velocity, and position of each node given the old velocity and position values using an explicit Euler solution with time step Δt [37], we have

$$\begin{aligned} A &= F./[MM] \\ V &= V^{old} + A\Delta t \\ P &= P^{old} + V\Delta t \end{aligned} \tag{5}$$

2.2.2. Physics-based Deformations

In order to traverse the image space, fit to specified regions, and take new shapes, a deformable organism must be able to undertake a sequence of spatial and shape based deformations. Some deformations take place independently of the topological design of the organism (general deformations), while others are designed specifically for medial-axis based worm type organisms (medial-based deformations). What follows is a description of the set of deformations comprising both scenarios.

General Deformations Many general deformations were introduced in [37], including bending, rotating, translating, scaling, bulging, stretching, and tapering. However, in this application we have only made use of rotating, translating and stretching deformations. Consequently what follows is a brief explanation of these three deformations, and an explanation of their application to our corpus callosum segmenting organism.

Rotation and translation are accomplished by applying a time decaying external force to all the nodes of a deformable organism. For rotation the direction of force at each node is consistently clockwise/counterclockwise and orthogonal to the line connecting that node with the organism's center of mass (figure 5a). However for translation the direction of force is constant across all nodes.

Stretching deformations apply spatially varying spring actuations designed to stretch the model locally in a specific direction. Given a center C, radius R, amplitude K, and direction D, a shape deformation takes place by actuating a spring s, if and only if one of its terminal nodes lies within the circular region defined by C and R (Figure 5.n). The new rest length r of spring s is calculated as

$$r = \left(\left(1 - \frac{d}{R}\right)\left(1 - \frac{2\theta}{\pi}\right)(K-1) + 1\right) r^{old} \tag{6}$$

where d is the distance from the midpoint of spring s to c, and θ is the angle between the stretching direction D and the spring s. Consequently, springs with direction and midpoint close to D and C, respectively, are affected more [37].

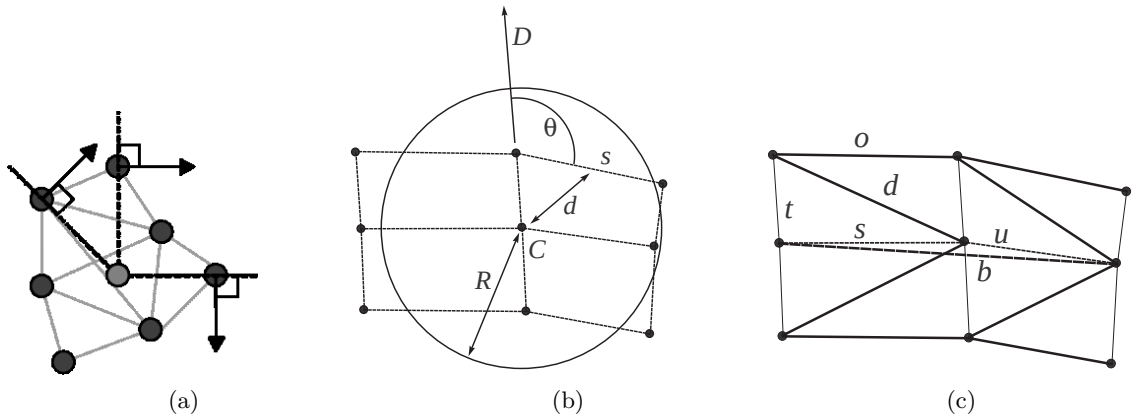

(a) (b) (c)

Figure 5. Physics based deformations. (a) Rotational forces. Definition of variables for (b) stretching and (c) contracting deformations.

For our purposes these general deformations were modified to apply to specific anatomical regions of the model. By fixing a group of nodes in place, we can perform deformations on specific regions of our corpus callosum model without affecting others. We use the terms regional rotation/translation, and boundary expansion to refer to these types of deformations. Boundary expansion refers to a sequence of stretching deformations whose direction is along thickness springs, while all nodes aside from the concerned boundary node are fixed.

Medial-Based Deformations The medial-based deformations include expansion, contraction, and medial alignment. Each can be executed across the entire organism, or across a small section, and can vary in strength, and duration.

Expansion deformations are an extension of the translation deformation. Given a set of neighboring medial nodes and an amplitude, a deformation is produced that consists of a sequential application of translational forces running from the first to last medial node in the range, and directed parallel to the medial axis. The forces are applied to the current medial node and its boundary nodes, while all nodes outside the expansion range remain fixed.

The contraction deformation is constructed through a sequence of spring actuations designed to shorten the medial length within a specific range. Given an amplitude K, a set of medial nodes M, and an amount of time to spend on each element of the range. The deformation begins by fixing the positions of all medial/boundary nodes from the second element of the range onward. Spring actuations are now carried out on all of the springs connecting medial/boundary nodes of the first range element to medial/boundary nodes of another element in the range. Suppose we have a particular medial node n, now we have a set of springs d,o,s,t,u,b as shown in figure 5.c, springs s,o are actuated by K. New rest lengths are calculated for d and b as follows

$$restlength_d = \sqrt{\left(K\left\|s\right\| + \left\|t\right\|\cos\left(\pi - \theta\right)\right)^2 + \left(\left\|t\right\|\cos\left(\theta - \frac{\pi}{2}\right)\right)^2} \tag{7}$$

$$\theta = \cos^{-1}\left(\frac{\left\|s\right\|^2 + \left\|t\right\|^2 - \left\|d^{old}\right\|^2}{2\left\|s\right\|\left\|t\right\|}\right) \tag{8}$$

where $\|x\|$ denotes the length of a spring x. For b simply replace d,t with b,u respectively. Clearly the same equations apply for the springs located below s in figure 5b. After a specific time the next set of medial/boundary nodes from the range is unfixed and the sequence is repeated.

The medial alignment deformation is also composed of an ordered progression of deformations across a range of medial nodes. Given an amplitude K, a time α and a range M, the deformation begins by fixing the positions

of all nodes in the model. Now suppose we are deforming on a particular medial node n, with thickness spring connected boundary nodes b_1, b_2. We unlock these three nodes, then apply a translational force to all three nodes going from b_2 to n, then after a time α we set the nodes back into their pre-deformation position and apply a translational force from b_1 to n. Lastly, we lock our three nodes, then begin deforming the next set in the range.

2.3. Behavioral Layer

The segmentation plan is sub-divided into different behavioral stages with sub-goals that are easy to define and attain (e.g. locating the upper boundary of an anatomical structure). The topmost cognitive layer of the architecture (section 2.5) combines prior anatomical knowledge, a segmentation plan, and an organism's sensory data (section 2.4) in order to initiate behaviors, carry out shape deformations, change sensory input, and make decisions towards segmenting the target structure. In the following subsections we describe the different behavioral routines necessary to achieve successful segmentation of the corpus callosum.

2.3.1. Model Initialization

In order to begin its search for the corpus callosum, the deformable organism must first be initialized to an appropriate location in the image using robust anatomical features. A modified hough transform [38] is first used to locate the largest ellipse corresponding to the skull in a midsagittal MRI slice. A template consisting of a rectangular window connecting two squares is used to approximate the main body, genu, and splenium of the corpus callosum (CC). Maximal average image intensity and minimal intensity variance are used as matching criteria. Several candidate locations for the three CC parts are identified and the set which exhibits the strongest edge-connectivity and exhibits maximal distance between the parts is selected.

2.3.2. Global Alignment

The global alignment phase is designed to find the best overall location for the model. Forces are applied to the entire organism to rotate and position it as necessary. The organism first locates the optimal horizontal/vertical location using translation forces, then finds the best alignment using rotation forces. Optimal translations are chosen using a position decision based upon a sensory module configured to monitor local image mean, and variance across the entire model. As the corpus callosum is generally a bright, homogenous region the decision function attempts to maximize the image mean, while minimizing the variance (more details presented in section 2.5.1).

2.3.3. Regional Alignment

During the regional alignment behavior, the organism aligns its anatomical parts to corresponding sections of the CC through successive phases. During each phase, rotational and translational forces are applied to only one part of the CC model. The phases are ordered as splenium-, genu-, and finally rostrum-alignment. This particular ordering favors segmenting regions with stable features before proceeding to other regions. Optimal positions are decided upon using a position decision function utilizing the same sensory module as mentioned in the previous section.

2.3.4. Expansion and Contraction

Since not all corpus callosum share the same medial length, it becomes necessary to expand/contract along the medial axis of the organism. As with earlier behaviors anatomically based phases are used to improve segmentation results. These regional phases are again the splenium, genu, and rostrum. Each region is first expanded/contracted along the organisms medial axis. Favorable positions are decided upon using a position decision function designed to maximize regional image mean, while minimizing regional image variance and organism area (section 2.5.1). Then for each region the organism must decide if further expansion/contraction is required (section 2.5.2). If not, each region is again rotated as it was during the regional alignment phase. Lastly, each region is expanded and contracted a final time to ensure an optimal fit using the position decision function as before.

2.3.5. Medial Alignment

Although the many deformations performed throughout the previous stages optimally place particular regions of the organism, they may not favorably place all parts of those regions. In order to provide accurate segmentation results, the position of each cross section of the deformable organism must now be optimized through a medial alignment deformation across all medial nodes. Optimization takes place in the form of a position decision that is made after each element of the range has been deformed, and is designed to maximize local image mean, while minimizing local image variance (section 2.5.1).

2.3.6. Fitting to Boundary

In order to fit to the boundary of the corpus callosum the organism must locate the optimal position of each boundary node. It is not valid to assume that a node is optimally placed if it simply lies upon an edge because the boundary continuity between nodes must also be accounted for. Consequently, the boundary expansion deformation (section 2.2.2) is carried out across all nodes in a sequential order, and the decision process takes form as a position decision which weights the local image mean, variance, and gradient, as well as the organisms volume (section 2.5.1). Its goal is to maximize image mean and gradient, while minimizing image variance and object volume.

2.3.7. Detecting and Repairing Segmentation Inaccuracies

An example of the organisms ability to incorporate anatomical knowledge is its ability to detect and repair the fornix dip. Typically, the anatomical structure of a corpus callosum exhibits a symmetrical property about its medial axis. Consequently, if the organism is non-symmetrical in the region where the fornix dip is located then that area needs repair. In order to repair itself, the organism simply mirrors its top half about the medial axis throughout the affected area. To ensure validity, the organism then checks if the deformation has been beneficial using a position decision function designed to maximize local image mean, and minimize local image variance (section 2.5.1).

2.4. Sensory Modules

In order to perceive its surroundings the organism can perform various sensory functions. Although each method obtains the initial image data in the same manner, they all evaluate different image features including mean, variance, and edge strength. Image data is obtained through low-level image processing consisting of first projecting the models outer contour onto the image, then sampling all image pixels contained within the projected boundary. Equivocally, one can create a filled binary mask of the model, then multiply the mask by the image. It now becomes possible to measure the image mean, variance and edge strength across the model. A sensory module also exists to return the actual image data, instead of a scalar value representing the result of some processing function.

2.5. Cognitive Layer

The cognitive layer is responsible for controlling the organism based on sensory input, prior anatomical knowledge, and a user provided schedule. This control takes form in the way of event/schedule driven actions, and sensory/knowledge based decisions. The actions are carried out by the behavioral layer (section 2.3), and simulated by the physics layer (section 2.2). Decisions are carried made at scheduled times according to user provided decision functions. Our organism can decide on the best position across a sequence of performed deformations, and whether or not to continue its expansion/contraction behavior. What follows is a description of each.

2.5.1. Position Decision

The position decision evaluates a user provided function across a sensory information set that has been created by capturing sensory input throughout the deformation process. Our decision functions minimize/maximize weighted combinations of sensory input after the deformations have concluded to find the globally optimal solution, and avoid allowing the organism to get stuck at local minima/maxima. An example decision function might maximize the mean, while minimizing the variance. Assume that m,v are $n \times 1$ column vectors representing n sensory samples of the mean, variance respectively. Then $d = \alpha m + (1 - \alpha)(1 - v)$ where $0 \leq \alpha \leq 1$. Now the

position corresponding to *max(d)* is one that maximizes the mean image intensity, while minimizing the variance according to a weight α. In other words this particular decision function causes the deformable organism to prefer bright homogenous regions like the corpus callosum over dim non-uniform regions.

2.5.2. Expansion/Contraction Decision

Due to the various shapes and sizes the corpus callosum can take from subject to subject some instances may require further expansion/contraction of the splenium/genu then others. Our organism makes this decision based upon sensory input localized to the concerned area. More specifically, if a single image edge is found to cross the model within the concerned area then further deformation is required.

3. RESULTS

We present qualitative as well as quantitative results of fully-automatic segmentation of the corpus callosum in mid-sagittal magnetic resonance images [39] (N=46) using the physics-based deformable organism (Figure 6). The organism's behaviors and awareness of the different stages of the plan enables it to not only segment the CC but also label anatomical regions (Figure 7(a)). We also present further improvement of the segmentation results (decrease in error) through minor, intuitive user interaction (Table 1 and Figure 7(b,c)).

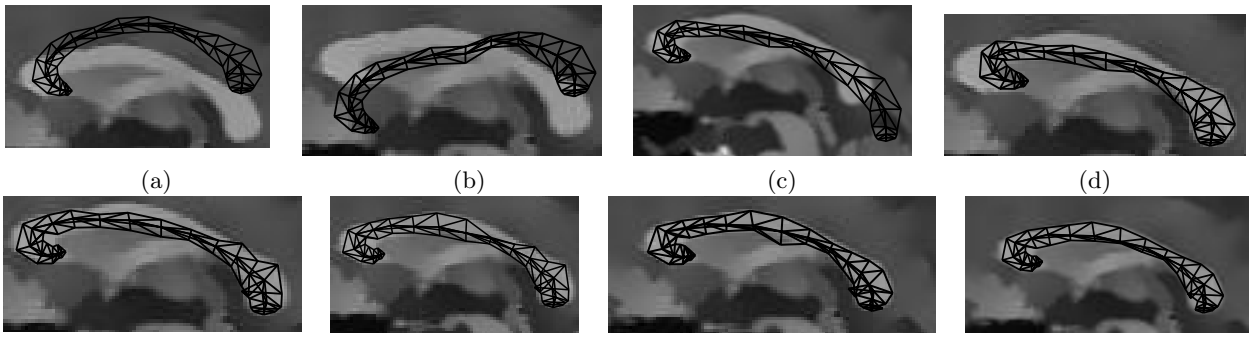

(a) (b) (c) (d)

(e) (f) (g) (h)

Figure 6. Progress of segmentation. (a) Global model alignment. (b) Model parts' alignment through (c) expansion and (d) contraction. (e) Medial-axis alignment. (f) Fitting to Boundary. (g) Detecting and (h) repairing the fornix dip.

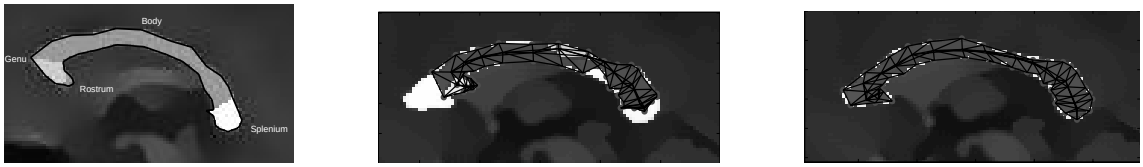

(a) (b) (c)

Figure 7. (a) Automatic labelling of important anatomical regions of the corpus callosum. (b) Before and (c) after intuitive manual intervention to improve the segmentation (white color corresponds to areas of erroneous segmentation).

4. CONCLUSIONS

We presented physics-based deformable organisms for segmentation, labelling, and quantitative analysis of medical image data. These organisms, which embody a medial-based geometry and are capable of controlled physics-based deformations, live in the image space and segment structures through the utilization of a segmentation plan of behaviors, prior anatomical knowledge, and perception of image data. Our results show that although automatic segmentation gives good results, the physics-based formulism allows the expert to provide real-time

Table 1. Error comparison before and after minor, intuitive manual intervention. Error $\varepsilon = (S \cup M - S \cap M)/M$ is used, where S and M denote the area enclosed within the result of the automatic segmentation and the manual expert delineation, respectively.

Error	**mean**	**median**	**min**	**max**	**std**
fully automated	0.1834	0.1706	0.1095	0.4526	0.0576
after minor user interaction	0.1009	0.0996	0.0561	0.1393	0.0174

guidance through minor intuitive interactions, if needed, which further improves the segmentation accuracy and keeps the expert "in-the-loop".

In earlier work deformable organisms relied on purely geometrical deformations which rendered intuitive, real-time user-interaction difficult to implement and also necessitated the incorporation of extraneous geometric constraints for maintaining the integrity of the deformable shape model. The primary contribution of this work is the incorporation of a physics layer into the deformable organisms framework thus circumventing the above problems. In this work we applied the physics-based deformable organisms framework to segment anatomical structures in real medical data and demonstrated the opportunity for manual expert intervention if needed.

5. ACKNOWLEDGEMENTS

GH was partly funded by NSERC (Natural Sciences and Engineering Research Council of Canada) discovery grant and Simon Fraser University Presidents Research Grant Fund. CM was funded by NSERC USRA (Undergraduate Student Research Award).

REFERENCES

1. T. S. Yoo, *Insight into Images: Principles and Practice for Segmentation, Registration, and Image Analysis*, A k Peters Ltd., suite 230, 888 Worcester St. Wellesey, MA, USA, 2004.
2. R. A. Robb, *Biomedical Imaging, Visualization, and Analysis*, Wiley-Liss Inc., 2000.
3. A. Dhawan, *Medical Image Analysis*, Willey-IEEEE Press, 2003.
4. I. Bankman, *Handbook of Medical Imaging: Processing and Analysis*, Academic Press, 2000.
5. M. Sonka and J. Fitzpatrick, *Handbook of Medical Imaging, Volume 2: Medical Image Processing and Analysis*, SPIE-International Society for Optical Engine, 2000.
6. D. Terzopoulos, "On matching deformable models to images," *Topical Meeting on Machine Vision, Technical Digest Series* **12**, pp. 160–167, 1987.
7. M. Kass, A. Witkin, and D. Terzopoulos, "Snakes: Active contour models," *International Journal of Computer Vision* **1(4)**, pp. 321–331, 1987.
8. T. McInerney and D. Terzopoulos, "Deformable models in medical image analysis: A survey," in *Medical Image Analysis*, **1(2)**, pp. 91–108, 1996.
9. J. Montagnat, H. Delingette, and N. Ayache, "A review of deformable surfaces: topology, geometry and deformation," in *Image and Vision Computing*, **19(14)**, pp. 1023–1040, 2001.
10. S. Osher and N. Paragios, *Geometric Level Set Methods in Imaging Vision and Graphics*, Springer Verlag, 2003.
11. V. Caselles, R. Kimmel, and G. Sapiro, "Geodesic active contours," in *International Journal of Computer Vision*, **22(1)**, pp. 61–79, 1997.
12. J. A. Sethian, "Level set methods; evolving interfaces in geometry, fluid mechanics," in *Computer Vision and Material Sciences*, Cambridge University Press, 1996.
13. L. D. Cohen, "On active contour models and balloons," *CVGIP: Image Underst.* **53**(2), pp. 211–218, 1991.
14. C. Xu and J. Prince., "Snakes, shapes, and gradient vector flow," **7(3)**, pp. 359–369, 1998.
15. T. F. Cootes, D. Cooper, C. J. Taylor, and J. Graham, "Their training and application," in *Computer Vision and Image Understanding*, **61**, pp. 38–59, 1995.

16. T. F. Cootes, G. J. Edwards, and C. J. Taylor, "Active appearance models," in *IEEE Transactions on Pattern Analysis and Machine Intelligence*, **23(1)**, pp. 681–685, 2001.
17. M. Leventon, E. Grimson, and O. Faugeras., "Statistical shape influence in geodesic active contours," in *Computer Vision and Pattern Recognition (CVPR)*, 2000.
18. S. K. Warfield, M. Kaus, F. A. Jolesz, and R. Kikinis, "Adaptive, template moderated, spatially varying statistical classification," in *Medical Image Analysis*, **4(1)**, pp. 43–55, 2000.
19. G. Hamarneh and T. Gustavsson, "Statistically constrained snake deformations," in *IEEE International Conference on Systems, Man, and Cybernetics*, **3**, pp. 1610–1615, 2000.
20. B. A. Draper, A. R. Hanson, and E. M. Riseman, "Learning blackboard-based scheduling algorithms for computer vision," in *International Journal of Pattern Recognition and Artificial Intelligence*, **7(2)**, pp. 309–328, 1993.
21. B. A. Draper, A. R. Hanson, and E. M. Riseman, "Knowledge-directed vision: Control, learning, and integration," in *IEEE Signals and Symbols*, **84(11)**, pp. 1625–1637, 1996.
22. D. Crevier and R. Lepage, "Knowledge-based image understanding systems: A survey," in *Computer Vision and Image Understanding*, **67(2)**, pp. 161–185, 1997.
23. T. Strat and M. Fischler, "Context-based vision: Recognizing objects using information from both 2-d and 3-d imagery," in *IEEE Transactions on Pattern Analysis and Machine Intelligence*, **13(10)**, pp. 1050–1065, 1991.
24. R. Poli, "Genetic programming for image analysis," in *Genetic Programming 1996: Proceedings of the First Annual Conference*, J. R. Koza, D. E. Goldberg, D. B. Fogel, and R. L. Riolo, eds., pp. 363–368, MIT Press, (Stanford University, CA, USA), 28–31 1996.
25. M. Martin, "Genetic programming for real world robot vision," in *IEEE/RSJ International Conference on intelligent Robots and Systems*, pp. 67–72, 2002.
26. J. Liu and Y. Tang, "Adaptive image segmentation with distributed behavior-based agents," in *IEEE Transactions on Pattern Analysis and Machine Intelligence*, **21(6)**, pp. 544–550, 1999.
27. L. Germond, M. Dojat, C. Taylor, and C. Garbay, "A cooperative framework for segmentation of mri brain scans," in *Artificial Intelligence in Medicine*, **20(1)**, pp. 77–93, 2000.
28. A. Boucher, A. Doisy, X. Ronot, and C. Garbay, "A society of goal-oriented agents for the analysis of living cells," in *Artificial Intelligence in Medicine*, **14**, pp. 183–199, 1998.
29. V. Rodin, F. Harrouet, P. Ballet, and J. Tisseau, "oris: Multiagents approach for image processing," in *SPIE Conference on Parallel and Distributed Methods for Image Processing II*, **3452**, pp. 57–68, 1998.
30. A. Bazen, M. van Otterlo, S. Gerez, and M. Poel, "A reinforcement learning agent for minutiae extraction from fingerprints," in *Proceedings of the Belgium-Netherlands Artificial Intelligence Conference (BNAIC'01')*, B. Kröse, M. de Rijke, G. Schreiber, and M. van Someren, eds., pp. 329–336, 2001.
31. G. Hamarneh, T. McInerney, and D. Terzopoulos, "Deformable organisms for automatic medical image analysis.," in *MICCAI*, pp. 66–76, 2001.
32. T. McInerney, G. Hamarneh, M. Shenton, and D. Terzopoulos, "Deformable organisms for automatic medical image analysis," *Medical Image Analysis* **6**(3), pp. 251–266, 2002. TY - JOUR.
33. D. Terzopoulos, X. Tu, and R. Grzeszczuk, "Artificial fishes: Autonomous locomotion, perception, behavior, and learning in a simulated physical world," *Artificial Life* **1**(4), pp. 327–351, 1994.
34. D. Terzopoulos, "Artificial life for computer graphics," *Commun. ACM* **42**(8), pp. 32–42, 1999.
35. G. Hamarneh, R. Abu-Gharbieh, and T. McInerney, "Medial profiles for modeling and statistical analysis of shape," *International Journal of Shape Modeling (in press)* .
36. G. Hamarneh and T. McInerney, "Controlled shape deformations via medial profiles," *Vision Interface* , pp. 252–258, 2001.
37. G. Hamarneh and T. McInerney, "Physics-based shape deformations for medical image analysis," *Image Processing: Algorithms and Systems II* **5014**(1), pp. 354–362, SPIE, 2003.
38. C. Kimme, D. H. Ballard, and J. Sklansky, "Finding circles by an array of accumulators," *Communications of the Association for Computing Machinery* **18**, pp. 120–122, 1975.
39. M. Shenton, R. Kikinis, F. Jolesz, S. Pollak, M. LeMay, C. Wible, H. Hokama, J. Martin, D. Metcalf, M. Coleman, and et al., "Abnormalities in the left temporal lobe and thought disorder in schizophrenia: A quantitative magnetic resonance imaging study," in *New England J. Medicine*, **327**, pp. 604–612, 1992.